



Analysis of the local domain size and the number of enriched nodes in a global-local GFEM approach simulating damage propagation in an L-shaped concrete panel

Anelize B. Monteiro¹, Felício B. Barros², Roque L. S. Pitangueira², Samuel S. Penna²

¹Federal University of Santa Catarina
8300 Dona Francisca St., CEP 89219-600, Joinville, SC, Brazil
anelize.m@ufsc.br

²Federal University of Minas Gerais
Federal University of Minas Gerais, 6627 Antonio Carlos Ave., CEP 31270-901, Belo Horizonte, MG, Brazil
felicio@dees.ufmg.br, roque@dees.ufmg.br, spenna@dees.ufmg.br

Abstract. The Generalized Finite Element Method (GFEM) has been developed to overcome some limitations inherent to the FEM by using some knowledge about the expected solution behavior to improve the analysis. The GFEM enriches the space of the polynomial FEM solution with *a priori* known information based on the concept of Partition of Unit. In this context, the GFEM global-local approach to the nonlinear analysis of quasi-brittle media is investigated here. The kernel concern is the impact on the structural global response of expanding the local domain and the number of nodes enriched with the global-local numerically obtained functions. Such analysis has been encouraged by observations that the quality of the global solution transferred to the boundary of the local problem can indeed impact the problem solution in media with linear elastic behavior. The importance of this is grounded by the interest in having a reasonably coarse global mesh to justify a global-local analysis with the local problem discretized by a fine mesh. It is suggested, for example, the polynomial enrichment of the initial global approximation and the increase in the size of the local domain, enlarging the so-called *buffer zone*. Here, this strategy is evaluated to solve nonlinear problems induced by the degradation of the continuous medium. Thereby, a Smeared Crack Model of fixed direction with the stress-strain laws of Carreira and Chu is applied in the local domain to simulate the damage propagation experimentally obtained in an L-shaped concrete panel. The resulting global-local responses are compared with experimental findings from the literature and numerical results obtained by standard GFEM.

Keywords: GFEM global-local, Continuous Damage Mechanics, Buffer zone

1 Introduction

The Generalized Finite Element Method (GFEM) has been developed to overcome limitations inherent to the FEM by using some knowledge about the expected solution behavior to improve the numerical responses. The application of GFEM to the nonlinear analysis of the damage and plasticity processes is established and other methods derived from GFEM have been conceived, such as the GFEM global-local. This method was proposed by Duarte and Babuška [1] and widely studied by Kim et al. [2], Freitas et al. [3] and Kim and Duarte [4]. Evangelista Jr et al. [5] proposed the formulation and development of GFEM global-local strategy which incorporates a Continuum Damage Model that uses scalar damage variable for quasi-brittle materials to simulate failure in mode I and mixed-mode crack propagation.

In Monteiro et al. [6] a global-local approach to the GFEM based on Kim and Duarte [4] was applied to describe the deterioration process of quasi-brittle media within the context of Continuous Damage Mechanics, by assuming the Smeared Crack Model of fixed direction with the stress-strain laws of Carreira and Chu [7] and Carreira and Chu [8] applied in the local domain to simulate the damage propagation experimentally obtained in an L-shaped concrete panel. As a continuation of the Monteiro et al. [6] investigations, in this paper the kernel concern is the impact on the structural global response of the number of nodes enriched with the global-local

numerically obtained functions and the increase in the size of the local domain, enlarging the so-called *buffer zone*.

This GFEM global-local approach was implemented by Monteiro [9] in the computational system `INSANE` (*INteractive Structural ANalysis Environment*) (Gori et al. [10]). This paper is organized as follows: in the Section 2 the implemented formulation is summarized, the Section 3 presents the numerical results obtained with the standard GFEM and GFEM global-local and the Section 4 discusses the responses obtained in the numerical simulations and suggests new analyses to be carried out to advance the investigations.

2 Formulation

This section briefly presents the formulation of the GFEM global-local implemented in the computational system `INSANE` system by Monteiro [9]. The numerical solution used to enrich the global problem is obtained through physically nonlinear analysis performed only in the local region. With the damage of the local region incorporated into the global problem, through the global-local enrichment functions, the linear analysis is performed in the global region. This process is carried out in blocks of global-local analysis able to capture the evolution of the deterioration process and their influence on the global behavior of structures. Therefore, each block of global-local analysis has three stages:

Stage 1. Initial and estimated linear global problem

For the initial linear global problem, step $k = 0$, the global domain is defined by $\bar{\Omega}_G = \Omega_G \cup \partial\Omega_G$ in \mathbf{R}^n . The vector field $\mathbf{u}_{G,0}^0$ is the approximate solution of the weak form of the initial global problem:

$$\int_{\Omega_G} \sigma(\mathbf{u}_{G,0}^0) : \varepsilon(\mathbf{v}_{G,0}^0) d\mathbf{x} + \int_{\partial\Omega_G^u} \mathbf{u}_{G,0}^0 \cdot \mathbf{v}_{G,0}^0 ds = \int_{\partial\Omega_G^\sigma} \bar{\mathbf{t}} \cdot \mathbf{v}_{G,0}^0 ds + \int_{\partial\Omega_G^u} \bar{\mathbf{u}} \cdot \mathbf{v}_{G,0}^0 ds, \quad (1)$$

where $\mathbf{v}_{G,0}^0$ are the test functions of the initial global problem, σ is the stress tensor, ε is the strain tensor, $\bar{\mathbf{t}}$ is the prescribed stress vector, and $\bar{\mathbf{u}}$ is the prescribed displacement vector.

The solution $\mathbf{u}_{G,0}^0$ is obtained for the entire load (load factor $\lambda = 1$) and then it is adjusted according to the size of the displacement step P_{DG} (predefined for the global problem in the control node). The load factor is obtained by:

$$\lambda^0 = \frac{P_{DG}}{u_{G,0,DC}^0}, \quad (2)$$

where $u_{G,0,DC}^0$ is a displacement component of the control node, obtained from eq. (1).

To $k \geq 1$, in the estimated linear global problem, $\mathbf{u}_{G,0}^k$ is estimated by the following expression, adapted from Kim and Duarte [4]:

$$\mathbf{u}_{G,0}^k = \frac{(k+1)}{k} \mathbf{u}_{G,0}^{k-1}. \quad (3)$$

Stage 2. Nonlinear local problem

The local problem is solved incrementally-iteratively in the local domain Ω_L . The local displacement vector \mathbf{u}_L^k is calculated by the following equation, which has boundary conditions from the initial global solution of the Stage 1.

$$\int_{\Omega_L} \sigma(\mathbf{u}_L^k) : \varepsilon(\mathbf{v}_L^k) d\mathbf{x} + \eta \int_{\partial\Omega_L \cap \partial\Omega_G^u} \mathbf{u}_L^k \cdot \mathbf{v}_L^k ds = \int_{\partial\Omega_L \cap \Omega_G^\sigma} \bar{\mathbf{t}} \cdot \mathbf{v}_L^k ds + \int_{\partial\Omega_L \setminus (\partial\Omega_L \cap \partial\Omega_G)} [\mathbf{t}(\mathbf{u}_G^k) + \eta \mathbf{u}_G^k] \cdot \mathbf{v}_L^k ds, \quad (4)$$

where η is the penalty parameter, \mathbf{v}_L^k are the test functions of the local problem, and $\mathbf{t}(\mathbf{u}_G^k)$ is the stress vector

In this stage of each block of global-local analysis, it is necessary to solve the problem from the beginning of the loading, up to the level of loading of the block. In order to adequately represent the problem, the number of local steps resolved at each block is increased. The number of total local steps (N_{LS}) solved in each block k is given by:

$$N_{LS} = N_{IL} + [(k+1)N_{AL}], \quad (5)$$

where N_{IL} is the number of initial local steps, and N_{AL} is the number of local steps added to each global-local block.

Stage 3. Enriched linear global problem

The constitutive relation is given by $\sigma = \mathbf{C}^s : \varepsilon$, where ε is the strain tensor and \mathbf{C}^s is the secant approximation of the constitutive tensor adopted in the balance of the global model and obtained considering the damage occurred in the local problem. In this stage, local solution \mathbf{u}_L^k is applied as extrinsic basis for enriching the global problem:

$$\{\phi_J\}(x) = \mathcal{N}_J(x) \times \mathbf{u}_L^k, \quad (6)$$

where J is referred to nodal points, \mathcal{N}_J is the PoU function of the initial global problem and \mathbf{u}_L^k is the local solution, named global-local enrichment function. The global enriched problem is defined by:

$$\int_{\Omega_G} \sigma(\mathbf{u}_G^k) : \varepsilon(\mathbf{v}_G^k) d\mathbf{x} + \int_{\partial\Omega_G^u} \mathbf{u}_G^k \cdot \mathbf{v}_G^k ds = \int_{\partial\Omega_G^\sigma} \bar{\mathbf{t}} \cdot \mathbf{v}_G^k ds + \int_{\partial\Omega_G^u} \bar{\mathbf{u}} \cdot \mathbf{v}_G^k ds, \quad (7)$$

The solution \mathbf{u}_G^k is obtained for the entire load (load factor $\lambda = 1$). \mathbf{u}_G^k is adjusted according to the size of the displacement step S_{GD} predefined for the global problem. The load factor λ_E^k is defined as:

$$\lambda_E^k = \frac{(k+1)S_{GD}}{u_{G,DC}^k}, \quad (8)$$

where $u_{G,DC}^k$ is a displacement component of the control node, obtained from eq.(7).

3 Numerical Simulations

The Smeared Crack Model of fixed direction with the Carreira and Chu [7] and Carreira and Chu [8] stress-strain laws, available in the library of constitutive models of INSANE, it is used in the numerical simulations of a L-shaped concrete panel in the local problem and in the standard GFEM analysis. In the global problem the material is initially linear elastic. To evaluate the impact on the structural global response of the number of nodes enriched with the global-local functions and the increase in the size of the local domain, the numerical results are compared to the experimental ones of Winkler et al. [11]. The concrete properties obtained by Winkler et al. [11] and the material parameters adopted are compiled in Monteiro et al. [6].

Figure 1(a) shows the geometry, loading and boundary conditions of these tests. The loading is distributed with the value of $q = 28.0$ N/mm and the panel thickness is 100 mm. In the global meshes the point A corresponds to the node whose vertical displacement is considered in the composition of the equilibrium paths. In the local mesh point B is adopted as a control node in the nonlinear analysis by the displacement control method.

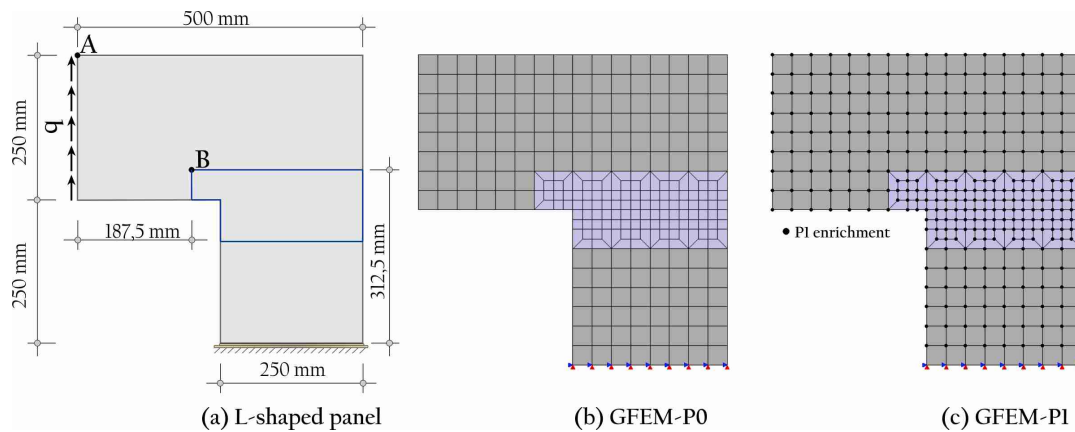


Figure 1. (a)L-shaped concrete panel; (b) and (c) Meshes evaluated with standard GFEM.

The nonlinear analysis of the local problem is performed with the displacement control method, secant approximation to the constitutive tensor and tolerance to convergence equals to $1 \times 10^{-5} (\times 100\%) = 0.0010\%$ in relation to the norm of incremental displacements vector. In local mesh, penalty parameter is $\eta = 1 \times 10^{10}$ and there are 4×4 Gauss points per element (same number in the global mesh).

The definition of numerical parameters of the GFEM global-local is based on the results obtained by Monteiro et al. [6]: 50 global steps, 10 initial local steps, 10 added local to each block of analysis, displacement global step of 0.02 mm, and displacement control method: point B in the vertical direction (Figure 1(a)).

In the L-panel [11] the initiation of the crack occurs at the angular joint of the panel and it propagates horizontally throughout almost the entire structure. For this reason, the global nodes chosen to be enriched with

the global-local solution are located in such a region. The number of global enriched nodes and the size of the local domain were varied to evaluate the influence on the obtained responses. Therefore, the following analyses are performed:

- 3.1: Standard GFEM without polynomial enrichment function (denoted by GFEM-P0) and with all nodes enriched by linear polynomial function (denoted by GFEM-P1); and
- 3.2: GFEM global-local with 9 and 29 nodes enriched by the global-local function, analysing the three local domains.

3.1 Standard GFEM: P0 and P1 enrichment function

As done by Kim and Duarte [4], the mesh used for the application of the standard GFEM has the same level of refinement of the local mesh that will be presented in the Section 3.2. The mesh shown in Fig. 1(b, c) has 281 elements and 316 nodes, GFEM-P0 has 632 degrees of freedom and GFEM-P1 has 3756 degrees of freedom. To maintain equivalence with the number of local steps in the last block of global-local analysis (block $k = 50$ with 510 local steps) of the simulations with global-local GFEM, it was adopted 500 steps and displacement control method of point A in the vertical direction (Figure 1(a)), with displacement steps of 0.002 mm.

In the Fig. 2 the behavior of the two equilibrium paths, whose peak loads remained below the limit value of the experimental results, suggests that there was strain localization. The presence of polynomial enrichment led to the greatest reduction in the peak load of the GFEM-P1 equilibrium path. From these observations, it is inferred that the global mesh refinement in the region of damage development and the solution with standard GFEM are unable to capture the structural behavior of the L-panel, and that the use of uniformly distributed polynomial enrichment for the entire domain deviates further the obtained responses from the experimental spectrum of Winkler et al. [11].

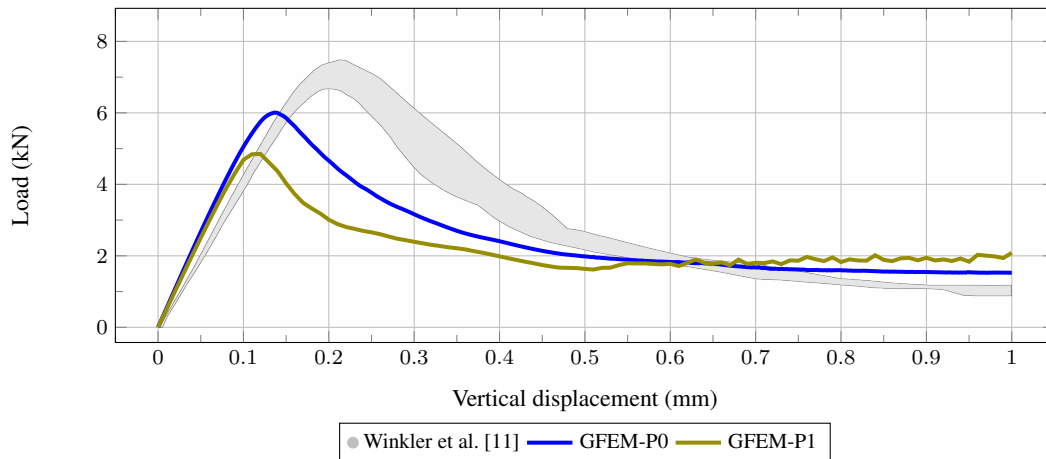


Figure 2. Equilibrium paths: standard GFEM P0 and P1

3.2 GFEM global-local: 9 and 29 enriched nodes

The global and local meshes are shown in the Fig. 3, such as the details the global nodes enriched with the local numerical solution for each analysed case: with 9 and 29 nodes. There are three domains in the global mesh that are equivalent to three local problems, specified by:

- Local problem 1 (blue): global domain with 36 elements, 125 local elements and 142 nodes;
- Local problem 2 (yellow): global domain with 57 elements, 146 local elements and 166 nodes; and
- Local problem 3 (pink): global domain with 80 elements, 169 local elements and 192 nodes.

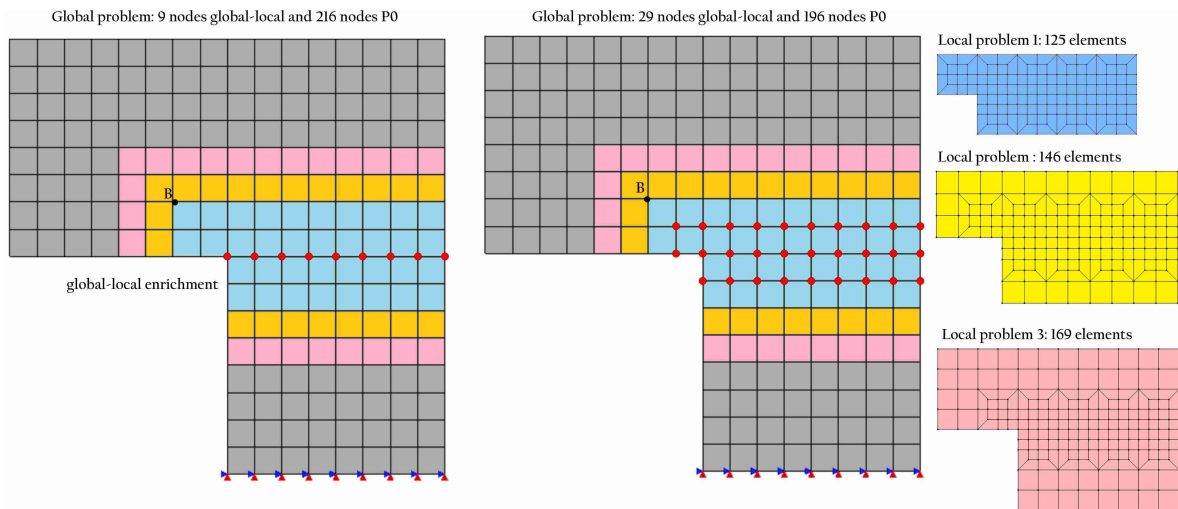


Figure 3. GFEM global-local meshes: 9 and 29 enriched nodes.

Three analyses were performed for the each local problems with 9 and 29 enriched nodes, generating the six equilibrium paths presented in Fig. 4. In general, it is noted that the application of the proposed GFEM global-local improved the responses obtained regarding the approximation of the peak loads to the experimental load limit and the adequate description of the equilibrium path, in relation to the results obtained with the standard GFEM in the Section 3.1.

Regarding the global problem with 9 enriched nodes, the convergence of the three paths is observed and the increase in the size of the local domain did not significantly affect the obtained responses. Thus, the 9 enriched nodes were sufficient to obtain responses very close to the experimental spectrum. The equilibrium paths with 29 enriched nodes became more flexible and the peak loads are lower than the experimental load limit, but following the trend of the experimental spectrum. When the domain is large enough to involve the damage process, the increase in the local domain does not influence the obtained responses, since the figure above shows the convergence of equilibrium paths for the three local domains.

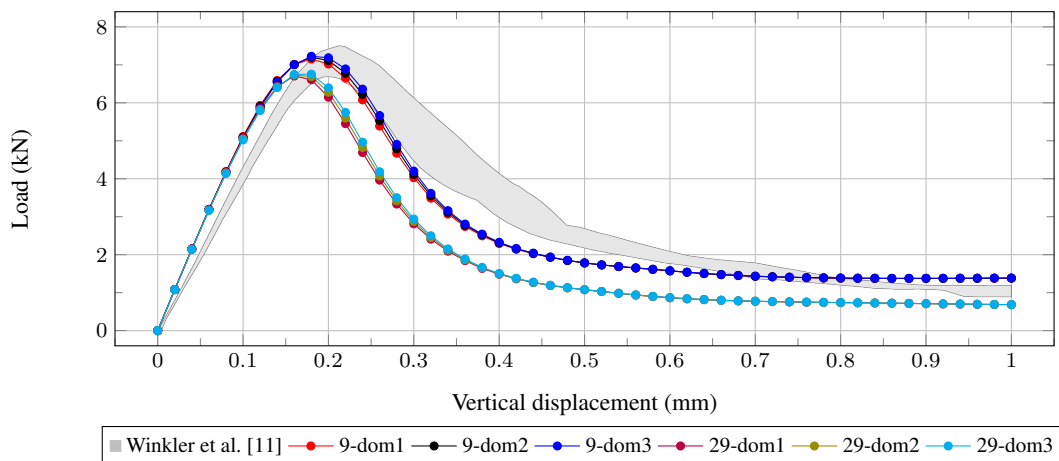


Figure 4. Equilibrium paths: GFEM global-local with 9 and 29 enriched nodes to the domains 1, 2 and 3.

The graphs representing the damage distribution by traction in the three local problems with 9 and 29 enriched nodes are gathered here as follows: local domain 1, 2 and 3 in the Figures 5, 6, and 7, respectively. The more pronounced damage with 29 enriched nodes is corroborated by the equilibrium paths of the Fig. 4, in which the same level of displacement is achieved at a lower load level than required for the 9 enriched nodes analyses. In the analysis block $k = 50$ of the three local problems, the damage advanced over two elements of the upper row in the analyses with 9 enriched nodes, which did not occur with 29 nodes, in which the damage remained concentrated on the central band of elements. This did not affect the results obtained, with the analyses with 9 enriched nodes leading to results consistent with the experimental results.

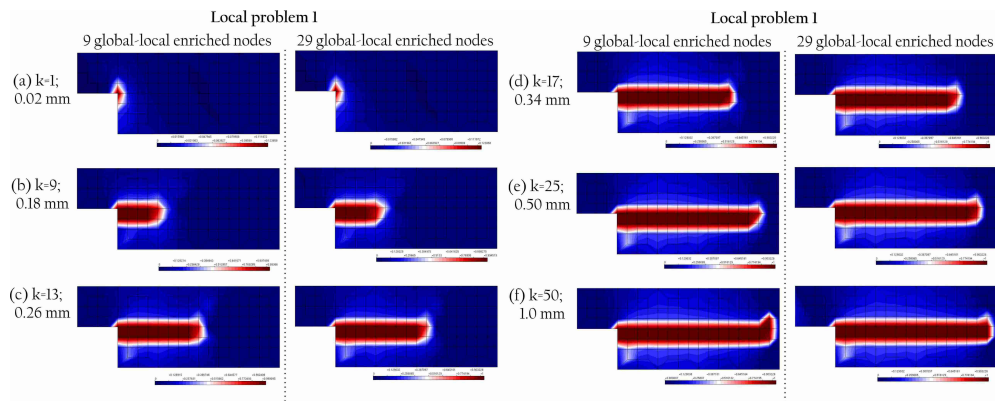


Figure 5. Damage process of the local problem 1: k blocks of global-local analysis.

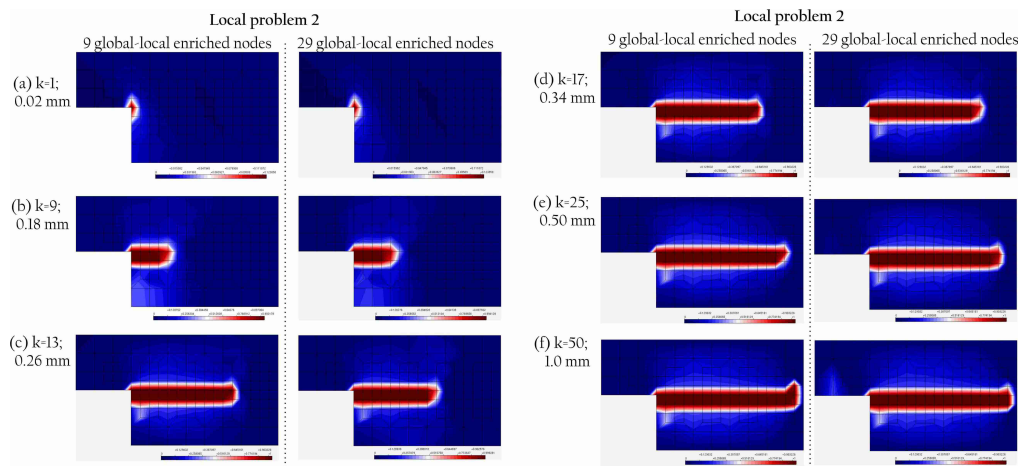


Figure 6. Damage process of the local problem 2: k blocks of global-local analysis.

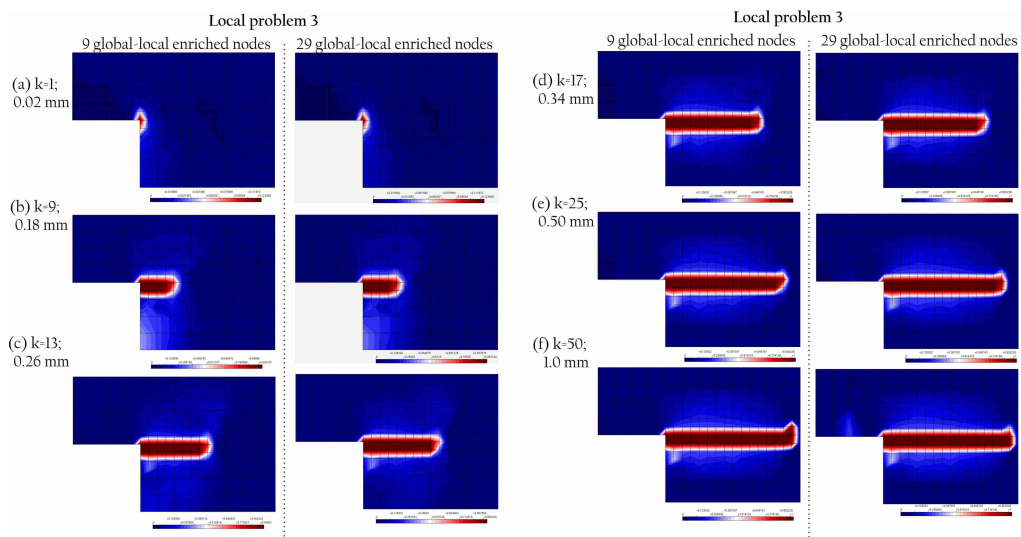


Figure 7. Damage process of the local problem 3: k blocks of global-local analysis.

4 Conclusions

According to [12], it is interesting to apply larger local domains since they would reduce the effect of the non-existence of exact boundary conditions to the local problems, but such greater domains are computationally expensive. However, in this paper is observed that the local domain 1 is sufficient to contain the damage evolution, being computationally less expensive than the domains 2 and 3, which have more elements to be analysed. It is observed that in domain 1 with 29 enriched nodes the *buffer zone* does not exist, which should be a problem based

on the literature data. Here, such failing is not identified presumably due to the fact that the damaged region is quite confined within the three domains, not impacting the quality of the boundary conditions that are applied from the result of the global problem.

Another typical aspect of the nonlinear analysis investigated here is the fact that the incremental process from the second block of global analysis of the global problem allows a higher quality approximation than the initial one. Gradually, at each block of global-local analysis, this global solution is incremented and the function to be imposed as a boundary condition in the local problem. This aspect can also be used to explain the reason for the size of the *buffer zone* has no impact on the quality of the local problem analysis. However, the use of 29 enriched nodes modifies the equilibrium paths indicating a similar trend of localization observed in the results obtained to the standard GFEM with polynomial enrichment function (Section 3.1). A more complete investigation will be presented in future works, in which the size and the refinement level of the local problem, and the number of enriched nodes in the global problem are considered.

Acknowledgements. The authors gratefully acknowledge the important support of the UFSC (Federal University of Santa Catarina) and of the Brazilian research agency CNPq (in Portuguese Conselho Nacional de Desenvolvimento Científico e Tecnológico - Grant 308444/2022-1) and FAPEMIG (in Portuguese Fundação de Amparo à Pesquisa de Minas Gerais - Grant APQ-01656-18).

Authorship statement. The authors hereby confirm that they are the sole liable persons responsible for the authorship of this work, and that all material that has been herein included as part of the present paper is either the property (and authorship) of the authors, or has the permission of the owners to be included here.

References

- [1] C. A. Duarte and I. Babuška. A global-local approach for the construction of enrichment functions for the generalized fem and its application to propagating three-dimensional cracks. *Technical report, ECCOMAS Thematic Conference on Meshless Methods*, vol. 06, n. 1, 2005.
- [2] D. J. Kim, C. Duarte, and S. P. Proença. A generalized finite element method with global-local enrichment functions for confined plasticity problems. *Computer Methods in Applied Mechanics and Engineering*, vol. 50, n. 1, pp. 563–578, 2012.
- [3] A. Freitas, D. A. F. Torres, P. T. R. Mendonça, and C. S. Barcellos. Comparative analysis of c^k - and c^0 - gfem applied to two-dimensional problems of confined plasticity. *Latin American Journal of Solids and Structures*, vol. 12, n. 5, pp. 861–882, 2015.
- [4] J. Kim and C. Duarte. A new generalized finite element method for two-scale simulations of propagating cohesive fractures in 3-d. *International Journal for Numerical Methods in Engineering*, vol. 197, n. 1, pp. 487–504, 2015.
- [5] F. Evangelista Jr, G. Alves, J. F. A. Moreira, and G. O. F. Paiva. A global–local strategy with the generalized finite element framework for continuum damage models. *Comput. Methods Appl. Mech. Engrg*, vol. 50, n. 1, pp. 1–20, 2020.
- [6] A. B. Monteiro, F. B. Barros, R. L. S. Pintangueira, and S. S. Penna. *Evaluation of Numerical Parameters of a global-local GFEM approach simulating damage propagation in a L-shaped concrete panel*, 2022.
- [7] D. J. Carreira and K. Chu. Stress-strain relationship for plain concrete in compression. *ACI Journal*, vol. 82, n. 1, pp. 797–804, 1985.
- [8] D. J. Carreira and K. Chu. Stress-strain relationship for reinforced concrete in tension. *ACI Journal*, vol. 83, n. 1, pp. 21–28, 1986.
- [9] A. B. Monteiro. *Análise não linear de meios parcialmente frágeis via abordagem global-local do Método dos Elementos Finitos Generalizados*, 2019.
- [10] L. . Gori, S. S. Penna, and R. L. S. Pitangueira. A computational framework for constitutive modelling. *Computers and Structure*, vol. 187, n. 1, pp. 1–23, 2017.
- [11] B. Winkler, G. Hofstetter, and H. Lehar. Application of a constitutive model for concrete to the analysis of a precast segmental tunnel lining. *International Journal for Numerical and Analytical Methods in Geomechanics*, vol. 28, n. 1, pp. 797–819, 2004.
- [12] C. A. Duarte and D. J. Kim. Analysis and applications of a generalized finite element method with global-local enrichment functions. *Computer Methods in Applied*, vol. 197, pp. 487–504, 2008.